

Hydrogen Peroxide Can Be a Plausible Biomarker in Cyanobacterial Bloom Treatment

Takashi Asaeda (✉ asaeda@mail.saitama-u.ac.jp)

Saitama University

Mizanur Rahman

Saitama University

Helayaye Damitha Lakmali Abeynayaka

Saitama University

Research Article

Keywords: stresses, photoinhibition and nutrient depletion, growth of cyanobacteria

Posted Date: June 30th, 2021

DOI: <https://doi.org/10.21203/rs.3.rs-650498/v1>

License: © ⓘ This work is licensed under a Creative Commons Attribution 4.0 International License.

[Read Full License](#)

Version of Record: A version of this preprint was published at Scientific Reports on January 7th, 2022.
See the published version at <https://doi.org/10.1038/s41598-021-02978-6>.

Abstract

The effect of combined stresses, photoinhibition and nutrient depletion, on the oxidative stress of cyanobacteria was measured in laboratory experiments, to develop the biomass prediction model. *Phormidium ambiguum* was exposed to various photosynthetically active radiation (PAR) intensities and phosphorous concentrations with fixed nitrogen concentration. The samples were subjected to stress assays by detecting hydrogen peroxide (H_2O_2) concentration and antioxidant activities of catalase (CAT) and superoxide dismutase (SOD). H_2O_2 concentration decreased to $30 \mu\text{molm}^{-2}\text{s}^{-1}$ of PAR, then increased further with higher PAR intensity. Regarding phosphorus concentration, H_2O_2 concentration generally decreased with increasing phosphorus concentration. SOD and CAT activities were proportionate to the H_2O_2 protein⁻¹. No H_2O_2 concentration detected outside of cells indicated the biological production of H_2O_2 , and the accumulated H_2O_2 concentration inside cells was parameterized with H_2O_2 concentration protein⁻¹. Over $30 \mu\text{molm}^{-2}\text{s}^{-1}$ of PAR, H_2O_2 concentration protein⁻¹ had a similar increasing trend with PAR intensity, independently of phosphorous concentration. Meanwhile, with increasing phosphorous concentration, H_2O_2 protein⁻¹ decreased in a similar pattern regardless of PAR intensity. Protein content decreased with increasing H_2O_2 gradually up to $4\text{nmol } H_2O_2 \text{ mg}^{-1}\text{protein}$, which provides a threshold to restrict the growth of cyanobacteria. With these results. an empirical formula was developed to obtain the cyanobacteria biomass.

Introduction

Cyanobacteria blooms often produce toxic metabolites and are harmful for other organisms as well as humans. Hydrogen peroxide (H_2O_2) is often endorsed to reduce the cyanobacterial abundance as it is more effective in application with cyanobacteria as compared to other phytoplankton¹⁻². However, H_2O_2 is also produced by other factors. First, hydrogen peroxide is generated photochemically from organic material exposed to UV, and H_2O_2 distribution was observed in natural lakes³⁻⁵. At the same time, H_2O_2 is biologically produced in cells, exposed to environmental stresses, including metal ion toxicity, salinization, temperature, PAR conditions, eutrophication, allelopathy, and pathogens. though its contribution with respect to the total concentration is unknown⁵.

Under a stress environment, endogenous reactive oxygen species (ROS) production, including superoxide, hydroxyl radicals and H_2O_2 exceeds its scavenging capacity⁶⁻⁸. Reactive oxygen species are important for growth regulation and signaling mechanisms in photosynthetic organisms⁹⁻¹⁰ and those organisms in turn are capable of controlling excess ROS production with their inherent scavenging enzymes and non-enzymatic components^{9,11}. Accumulation of an excessive amount of ROS inside cells causes harmful impacts on cyanobacteria such as disrupting the cellular homeostasis, causing membrane lipid peroxidation, protein oxidation, enzyme inhibition and DNA and RNA damages, etc., and affects the photosynthetic apparatus, finally leading to cell mortality as the concentration exceeds the threshold value¹².

Cyanobacteria are sensitive to even a minor change in light intensity as they usually expose relatively weak light, and thus even a moderate solar radiation may cause stress¹³. Collecting solar energy at photosystem II (PSII) in the thylakoid membrane results in the oxidation of water molecules and the reduction of plastoquinone, a molecule involved in the electron transport chain. The produced electrons are transported to PSI, where they are consumed in the synthesis of carbohydrates. An overabundance of solar energy, however, results in the generation of ROS, including superoxide radicals, as the energy transfer rate is limited due to the underutilization of energy absorbed by the PSII antenna complex in the PSII reaction center^{11,14-16}. Superoxide dismutase (SOD) catalyzes superoxide radicals into hydrogen peroxide (H₂O₂), before being detoxified into water by antioxidant activities¹⁷. However, the high oxidation potential of ROS can lead to the destruction of proteins, which otherwise recover the photosystem activities¹⁸. Thus, excessive solar radiation inhibits the proliferation of cyanobacteria. The shortage of nutrient conditions is also identified as a dominant stressor that suppresses the growth of cyanobacteria¹⁹. The combined effect of various abiotic stresses on the production rate is often reported²⁰⁻²¹. Some combinations inhibit growth due to contradicting effects of stressors; however, significant reduction of biomass is also reported as caused by simultaneous exposure to multiple stressors as compared to a single source of stress²².

The concentration of H₂O₂ and activity of antioxidant enzymes are some of the biomarkers employed in stress detections; and the role of H₂O₂, in plants and how they respond to environmental stress has been a focus throughout the literature²³⁻²⁵ suggesting a potential to develop ROS-based strategies for the prediction of cyanobacterial bloom formation and H₂O₂ concentration²⁶. Thus, this research was designed to study (1) effects of the PAR regime and phosphorus concentration on the stress of cyanobacteria, particularly H₂O₂ concentration, (2) the combined effects of the PAR regime and phosphorous concentration on H₂O₂ concentration, and (3) the relationship between H₂O₂ concentration and antioxidant enzyme activities of cyanobacteria, aiming at the possibility of applying H₂O₂ concentration as a proxy to detect stress intensity in algal management and the contribution rate of biological H₂O₂ production rate in the treatment.

Analyses

Total soluble protein content analysis

Total soluble protein concentration was determined by using the same method that was mentioned in²⁷ with minor modifications. Cyanobacterial cells were extracted from 1 mL of culture media by centrifugation at 4 °C for 10 min at 10,000 rpm, and the pellet was washed once with distilled water. Then, the cell pellet was subjected to a freeze-thaw cycle. Total soluble protein was extracted using 0.5 M NaOH solution, and the extraction was centrifuged at 4 °C for 20 min at 10,000 rpm. The supernatant was used as crude protein extract, and the protein content was quantitatively analyzed with the aid of Coomassie Bradford protein assay kit. Crude protein extract was stained with Coomassie (G-250) dye and

incubated for 10 min at room temperature, and then the absorbance was measured at 595 nm using a UV-Vis spectrometer (Shimazu, Japan). Protein content was determined using a known concentration series of Albumin.

Stress assay

H₂O₂ Assay

Cellular H₂O₂ contents were estimated according to the titanium chloride method²⁸. A total of 750 µL of 0.1% titanium chloride in 20% H₂SO₄ (v/v) was then added to initiate the reaction. The optical absorption after 1 min was measured at 410 nm using a spectrophotometer (UVmini-1240). However, the absorption at 410nm includes the effect of other soluble compounds²⁹⁻³¹. Thus, the H₂O₂ concentration was calculated from the slopes of the standard curve obtained from known H₂O₂ concentration, which was offset derived by the intercept absorption rate with zero H₂O₂ concentration samples³⁰. The results were compared with those of the e-FOX method and the suitable agreement was obtained³¹.

CAT assay

The CAT activity was measured by reacting 15 µL of 750 mM H₂O₂, 920 µL of potassium phosphate buffer, and 65 µL of extract supernatant. Optical absorption was measured at 240 nm using UV mini-1240. The measurements were recorded every 20 s for 3 min, and CAT activity was calculated using an extinction coefficient of 39.4 mM⁻¹cm³². Scavenging rate of H₂O₂ by enzyme extract per minute was defined as one unit of CAT per 1 µg of protein.

APX assay

For APX assay, the reaction mixture contained 100 µL of enzyme extract, 200 µL of 0.5 mM ascorbic acid in 50 mM potassium phosphate buffer (pH 7.0), and 2 mL of 50 mM potassium phosphate buffer (pH 7.0) was mixed with 60 µL of 1 mM H₂O₂. The decrease in absorbance at 290 nm was recorded every 20 s for 3 min. The APX activity was calculated using an extinction coefficient of 2.8 mM⁻¹ cm⁻¹ ³³.

SOD assay

Total SOD activity was determined by using methods as described by³⁴. The reaction mixture contained 50mM phosphate buffer (pH 7.8), 0.66 mM EDTA, 10 mM methionine, 33 µM NBT, 0.0033 mM riboflavin and 50 µL cyanobacterial enzyme extract. The reaction was allowed to proceed under a fluorescent illumination, after that the absorbance of the reaction mixture was read at 560 nm. One unit of SOD activity was defined as the amount of enzymes required to cause 50% inhibition of the NBT photo-reduction, and the results were expressed as unit per µg⁻¹ of total soluble protein.

Statistics

Variance (ANOVA) and the bivariate analysis were used and Pearson's correlation method was followed to evaluate the relationship among parameters. Statistical analyses were performed with the help of IBM SPSS V25.

H₂O₂ concentration showed correlations with increasing PAR intensities and decreasing phosphorus concentrations, independently. The fitted curve patterns were different for each PAR intensity or each phosphorous concentration.

Therefore, the most fitted curves of H₂O₂ concentration with respect to phosphorus concentration, and with respect to PAR intensity, 30 to 200 $\mu\text{molm}^{-2}\text{s}^{-1}$, were obtained for each PAR intensity, and the phosphorus concentration, 0.1 to 1000 mgL^{-1} , respectively, then the effect of PAR intensity and phosphorus concentration in the H₂O₂ concentration was estimated.

The variance (ANOVA) and the bivariate analysis were used and Pearson's correlation method was followed to evaluate the relationship among parameters. Statistical analyses were performed with the help of IBM SPSS V25.

Results

The effect of PAR intensity and phosphorous concentration on the H₂O₂ concentration

Protein content and H₂O₂ concentration are shown in Fig1. Protein content for different PAR intensity levels and for each phosphorus concentration level (mgL^{-1}). Vertical bars indicate standard deviation and Fig2. H₂O₂ concentration for different PAR intensity levels and for each phosphorus concentration level (mgL^{-1}). Vertical bars indicate standard deviation. with respect to PAR intensity.

Protein content was higher in less than 50 $\mu\text{molm}^{-2}\text{s}^{-1}$ of PAR, and was observed to increase with increasing PAR intensity; H₂O₂ concentration per protein shows the similar variational trend with respect to the PAR intensity Fig. 3. H₂O₂ content per protein for different PAR intensity levels and for each phosphorus concentration level (mgL^{-1}). Vertical bars indicate standard deviation. Regardless of phosphorous concentration, it declined with low PAR intensities down to 30 $\mu\text{molm}^{-2}\text{s}^{-1}$ of PAR intensity and then increased gradually with decreasing enhancement rate. At values higher than 50 $\mu\text{molm}^{-2}\text{s}^{-1}$ PAR, no significant difference with different phosphorus concentration levels was detected.

H₂O₂ per protein was generally lower with higher phosphorus concentration ($p < 0.03$) Fig. 4. H₂O₂ content per protein for different phosphorus concentration level (mgL^{-1}) and for each PAR intensity level ($\mu\text{molm}^{-2}\text{s}^{-1}$). Vertical bars indicate standard deviation. Dotted lines show the approximate relation for each light intensity.

H₂O₂ per protein, which was measured as high as 2.5 up to 10 $\mu\text{molm}^{-2}\text{s}^{-1}$, with 100 to 200 $\mu\text{molm}^{-2}\text{s}^{-1}$ of PAR intensities, declined with higher phosphorus concentration Fig. 4. H₂O₂ content per protein for

different phosphorus concentration level (mgL^{-1}) and for each PAR intensity level ($\mu\text{molm}^{-2}\text{s}^{-1}$). Vertical bars indicate standard deviation. Dotted lines show the approximate relation for each light intensity.

Fig. 3. H_2O_2 content per protein for different PAR intensity levels and for each phosphorus concentration level (mgL^{-1}). Vertical bars indicate standard deviation denotes the relationship between H_2O_2 per protein and PAR intensity for higher than $30 \mu\text{molm}^{-2}\text{s}^{-1}$ of PAR intensity. For all phosphorus concentration levels, H_2O_2 per protein values had a similar pattern with respect to PAR intensity ($p < 0.01$).

Antioxidant activities with respect to H_2O_2 concentration per protein

SOD activity was uniquely proportionate to H_2O_2 per protein Fig. 5. SOD activity per protein for different phosphorus concentration level (mgL^{-1}) and for each PAR intensity level ($\mu\text{molm}^{-2}\text{s}^{-1}$). The approximate relation is shown by the diagonal line, where $\text{H}_2\text{O}_2/\text{protein}(\text{nmolmg}^{-1}) = 0.176(\text{min}) * \text{SOD}(\text{nmolmg}^{-1} \text{min}^{-1})$, ($R^2 = -0.805$, $p < 0.01$).

CAT activity is shown as a function of H_2O_2 concentration per protein, separately shown by each phosphorous concentration Fig. 6. CAT activity per protein for different phosphorus concentration levels (mgL^{-1}). and for each PAR intensity level ($\mu\text{molm}^{-2}\text{s}^{-1}$). Dotted lines indicate the approximate lines for each phosphorus concentration. Overall CAT activity has a high correlation with H_2O_2 ($n=90$, $R^2=0.60$, $p < 0.01$).

For each phosphorus concentration level, CAT activity per protein linearly increased with $\text{H}_2\text{O}_2/\text{protein}$, and the increasing rate was higher based on PAR intensity ($18.73\text{CAT}/\text{H}_2\text{O}_2$, $R^2=0.573$ for 1000mgPL^{-1} , $13.82\text{CAT}/\text{H}_2\text{O}_2$, $R^2=0.977$ for 100mgPL^{-1} ; $12.89\text{CAT}/\text{H}_2\text{O}_2$, $R^2=0.793$ for 10mgPL^{-1} ; $14.53\text{CAT}/\text{H}_2\text{O}_2$, $R^2=0.949$ for 1mgPL^{-1} ; and $9.22\text{CAT}/\text{H}_2\text{O}_2$, $R^2=0.766$, for 0.1mgPL^{-1}), and the proportional coefficient was found to have a significant positive correlation with the logarithmic scale of the phosphorus concentration ($p < 0.01$).

For each PAR intensity level, on the other hand, CAT activity did not have significant positive correlation with the phosphorous concentration level.

Discussion

The effect of biologically produced H_2O_2 on the suppression of cyanobacterial blooms

The artificial endorsement of H_2O_2 has a high potential to suppress cyanobacterial blooms with less effects on other organisms compared to other controlling methods³⁵⁻³⁹. Researchers obtained the lethal H_2O_2 concentration of cyanobacteria by laboratory incubations under different concentrations of H_2O_2 ; cyanobacterial chlorophyll declined to nearly half after 18 h with the dose of approximately 30mmol of $\text{H}_2\text{O}_2 \text{L}^{-1}$ ^{1,40} and in 4 h with 100mmol of $\text{H}_2\text{O}_2 \text{L}^{-1}$ ². H_2O_2 delayed fluorescence decay with 0.1mmol of

H_2O_2 L^{-1} ³⁷, while the Fv/Fm value substantially declined with 100 mmol of H_2O_2 L^{-1} ⁴¹, dead cells increased with 275 mmol of H_2O_2 L^{-1} ³⁹. Cyanobacteria were in the lethal condition¹⁻² and sub-lethal at concentrations exceeding 50 mmol of H_2O_2 L^{-1} ³⁹. All experimental results reveal that cyanobacterial biomass is degraded with higher H_2O_2 concentration; however, the threshold H_2O_2 concentration varies widely from 1 to 1000 mmol L^{-1} .

Natural H_2O_2 formation has been identified in aquatic ecosystems as a photolysis of dissolved organic carbon (DOC) exposed to UV^{3,42-44} reported that the H_2O_2 production varies with the nutrient content of the water body. However, the H_2O_2 concentration of these waters was in the magnitude of mmol L^{-1} ^{4,26,45}. The comparison of these results indicates that the photolysis of organic carbon in natural water only is not sufficient to control cyanobacterial biomass.

H_2O_2 is also produced biologically and is accumulated in cells, subject to high levels of environmental stress. In the present experiment, UV was limited. Accordingly, measured H_2O_2 was considered a biologically produced component in cells or cell surfaces, which was then released into the ambient water. In the present experiment, protein content was measured as a reference of biomass of cyanobacteria. Cell biomass is two to three times larger with the protein content⁴⁶.

As the buoyancy of the cells is nearly neutral, the H_2O_2 content per protein, ~ 1 mmol of H_2O_2 kg^{-1} was generated and contained in the cell before release. This constitutes more or less the same level of the lethal H_2O_2 concentration in water.

The protein content in water declined with increasing H_2O_2 concentration per protein up to 2 nmol mg^{-1} protein. A higher protein level was not observed with higher H_2O_2 concentration levels in the present study. The growth of cyanobacteria is suppressed by the generation of higher H_2O_2 levels.

The lethal H_2O_2 concentration obtained here corresponds well with about 5 mmol of H_2O_2 g^{-1} FW of a threshold condition to grow *Egeria densa* in natural water²⁵, considering the weakness of cyanobacteria to H_2O_2 rather than other plant species³⁵.

The possible indicator of environmental stress and the effect of combined stress factors

The accumulation of ROS is reported to augment in parallel fashion to increased abiotic stress⁴⁷⁻⁴⁹. In the present experiment, two types of abiotic stresses, phosphorous deficiency and high or low PAR intensities were applied with different intensities of each.

Though H_2O_2 is produced under normal environmental conditions, their production is accelerated under high stress intensity. In natural water, cyanobacteria often suffer from a shortage of nitrogen and phosphorus. Stoichiometrically, the ratio of nitrogen and phosphorus of cyanobacterial cells is approximately 16:1 ⁵⁰. Waters with an N:P ratio of < 15 are most susceptible to cyanobacterial

dominance⁵¹⁻⁵². In the present experiment, the phosphorus concentration was changed with the fixed amount of nitrogen concentration of 3000mg L⁻¹. Thus, phosphorous concentration becomes restrictive, except for 1000mg P L⁻¹ in the present study's conditions. A significant increasing trend was observed in H₂O₂ per protein with decreasing phosphorus concentration. The deficiency of restrictive nutrients may increase the oxidative stress and then deteriorate the growth rate.

Under all tested phosphorus concentrations, H₂O₂ per protein content decreased with increasing PAR intensity until 30 μmolm⁻²s⁻¹, taking the lowest value there, then increased at higher PAR intensities though increasing rate gradually decreased. The enhanced production of H₂O₂ under prolonged low PAR conditions has not been reported upon sufficiently, though the production of superoxide in dark conditions is reported²⁶. With submerged macrophytes, *Egeria densa*, H₂O₂ concentration was empirically the lowest under the prolonged exposure of a PAR intensity level of approximately at 60 μmolm⁻²s⁻¹⁵³ and increased both with decreasing or increasing PAR intensities. However, the underlying mechanisms are unknown.

Increasing H₂O₂ concentration per protein over 30 μmolm⁻²s⁻¹ of PAR intensity is attributed to the excessive harvesting of PAR energy¹⁷⁻¹⁸. In the thylakoid membrane, electrons are produced by solar energy and transmitted to plastoquinone in PSII, which are partially accepted for the carbon dioxide fixation. More electrons are generated, when exposed to higher levels of solar radiation, and consequently, the photoinhibition of photosystem-II (PS-II) is induced, leading to oxidative damage because of the generated ROS, such as superoxide, hydroxyl radical, and H₂O₂. It damages cellular components, such as D1 protein, which otherwise mends the damaged photosynthesis apparatus¹⁸.

The process is composed of the direct reduction of O₂ by PS-I resulting in the production of singlet oxygen, followed by superoxide, which is converted to H₂O₂ by the activities of the enzyme SOD.

In the present study, H₂O₂ per protein was proportionate with SOD activity, which generates H₂O₂ from superoxide. CAT activity was far higher than other major antioxidant activities to decompose H₂O₂, and linearly increased with H₂O₂ concentration.

Though SOD and CAT activities demonstrated different dependencies on PAR intensity levels and the phosphorus concentration, their activities were evaluated by the single function with H₂O₂ per protein. The steady H₂O₂ concentration is sustained by the balance of the generated H₂O₂ by different type of stresses and these antioxidant activities, as a single function of H₂O₂ content per protein.

In natural water, cyanobacteria are exposed to various types of abiotic stresses that enhance the oxidative stress, producing H₂O₂, and it may deteriorate cyanobacterial biomass. Significant negative correlation was recognized for protein content with respect to H₂O₂ concentration (n=90, R²=-0.712, p<0.01), irrespective of stress types.

The production rate of H₂O₂ is not necessarily cumulative for different types of abiotic stresses²². However, H₂O₂ concentration was enhanced with increasing PAR intensity and decreasing phosphorus concentration, respectively, and the enhancement of H₂O₂ concentration was independent of each other (p<0.01). The total H₂O₂ per protein is empirically given as the sum of the amount of H₂O₂ produced by the intensity of each stress component, at least as a practical use level. Thus, for the combined stresses, the total H₂O₂ concentration is approximately provided by the sum of the H₂O₂ concentration attributed to each stress. The same trend was obtained for submerged macrophytes^{25,53}. Consequently, the potential to use the H₂O₂ concentration to estimate the cyanobacterial biomass exists.

The estimation of H₂O₂ concentration produced by cyanobacteria under abiotic stresses

For the application of the empirically obtained results to practical use in the prediction of algal blooms in the environment where PAR and phosphorous concentration, P, are restricted factors for the growth, the trend of the H₂O₂ per protein (nmol/mg) is obtained as a function of PAR (μmolm⁻²s⁻¹) and the phosphorous concentration, P (mgL⁻¹), as formulated by

$$\text{H}_2\text{O}_2/\text{protein} = -312 \cdot \text{PAR}^2 / (50^2 + \text{PAR}^2) \cdot ((25/\text{PAR})^4 + 1) \cdot \text{Log}(P/133100) \quad (1)$$

Where 0.1mg P L⁻¹ < P < 1000mg P L⁻¹, and 30 μmolm⁻²s⁻¹ < PAR, and protein represents the amount of protein in mgL⁻¹.

The relationship is shown in Fig. 8. The simulated results of H₂O₂/protein by equation (1) compared with experimental results and a significant similarity was obtained (R²=0.953, p=0.012, for 1000mg P L⁻¹, R²=0.696, p=0.0065 for 100 mg P L⁻¹; R²=0.927, p=0.023 for 20 mg P L⁻¹; R²=0.982, p=0.00289 for 1 mg P L⁻¹; R²=0.024, p=0.024 for 0.1 mg P L⁻¹).

The protein content (mgL⁻¹), as shown in Fig. 9. The simulated results of protein content by equation (2), as a function of H₂O₂ per protein was shown to possess significant negative correlation (R²=-0.675, p<0.01), which is empirically formulated by

$$\text{protein} = -192 \cdot \text{Log}((\text{H}_2\text{O}_2/\text{protein})/4.1) \quad (2)$$

(R²=-0.71, p<0.01).

With equation (1) and (2), protein content is estimated as a function of PAR and the phosphorous concentration.

The estimated protein contents are denoted in Fig. 7. Protein content in water for different phosphorus concentration levels (mg/L) and for each PAR intensity level (μmolm⁻²s⁻¹). The concentration uniquely increased with increasing phosphorus concentration.

The cellular growth rate gradually decreased with light intensity⁵⁴, and the growth rate of cyanobacteria reached a maximum at 30 to 50 $\mu\text{molm}^{-2}\text{s}^{-1}$ ⁵⁵. *P. ambiguum* prefers relatively low light intensity, at $\sim 18 \mu\text{molm}^{-2}\text{s}^{-1}$ ⁵⁶. The diagram seems to provide reasonable results.

Conclusions

Endogenous H_2O_2 concentration is an effective tool to detect the stress level of cyanobacteria.

Both PAR regimes and shortage of phosphorus concentration are shown to enhance H_2O_2 concentration in a cyanobacterial culture.

H_2O_2 per protein content declines in low PAR conditions, then increases when exposed to higher PAR intensity levels while generally increasing as phosphorus concentration decreases.

H_2O_2 per protein for combined stresses is given by the sum of the amount produced by each stress. Protein content decreases uniquely following the value of H_2O_2 per protein in a cyanobacterial culture. The prediction model was developed for the protein content, to design management criteria for excessive cyanobacterial blooms in freshwaters.

Methodology

Culture and Incubation

Phormidium ambiguum, which is an odor-forming benthic cyanobacterial species, was obtained from the National Institute of Studies (NIES), Japan. The strain was cultured and acclimatized for 30 days in an autoclaved BG 11 medium⁵⁷, maintained at 20°C under controlled PAR conditions with white fluorescent light, having flux of 20 $\mu\text{molm}^{-2}\text{s}^{-1}$ in a light-and-dark cycle of 12h:12h. The cultures were manually shaken twice a day. Cells were subcultured by diluting with new BG 11 medium as needed²⁷⁻²⁸.

Long-term exposure experiment

After 30 days, well-grown cyanobacterial cells were collected by centrifugation, washed once with distilled water, and then re-suspended in modified BG 11 media. All experiments were conducted by using incubators (MIR-254, Sanyo, Tokyo, Japan) with a nutrient level of BG-11 medium, consisting of NaNO_3 17.6 mM, K_2HPO_4 0.2296 mM, $\text{MgSO}_4 \cdot 7\text{H}_2\text{O}$ 0.0146 mM, Na_2CO_3 0.0189mM, Citric acid 0.0031 mM, Ferric ammonium citrate 0.0023 mM, EDTA (Na_2 salt) 0.0297 μM , H_3BO_3 4.6253 μM , $\text{MnCl}_2 \cdot 4\text{H}_2\text{O}$ 0.9145 μM , $\text{ZnSO}_4 \cdot 7\text{H}_2\text{O}$ 0.0765 μM , $\text{Na}_2\text{MoO}_4 \cdot 2\text{H}_2\text{O}$ 0.1611 μM , $\text{CuSO}_4 \cdot 5\text{H}_2\text{O}$ 0.0316 μM , and $\text{Co}(\text{NO}_3)_2 \cdot 6\text{H}_2\text{O}$ 0.0023 μM in 1 L of deionized water⁵⁷, adjusted for nitrogen and phosphorus concentrations respectively at 3000 mgL^{-1} of nitrogen and 0.1, 1.0, 10, 100, and 1000 mgL^{-1} of phosphorus. Six different PAR intensities, namely - 10, 20, 30, 50, 100 and 200 $\mu\text{molm}^{-2}\text{s}^{-1}$ by white fluorescent light (Toshiba, Japan) and VBP-L24-C2 PAR source (Valore, Kyoto, Japan) were used with

12h:12h PAR and dark cycle. The PAR intensities were measured using a quantum sensor (EKO Instruments Co., Ltd., Japan) and adjusted uniformly in the media. The temperature was kept constant (20 °C) throughout the experiment. At 12:00, after 7 days, samples were taken for the subsequent stress response analysis. Collected samples were subjected to bioassays that are described later.

Short-term (one day) exposure experiment

Another experimental setup was conducted to check the transition within a day of the culture. Above culture was exposed to 0, 30, 100, and 300 $\mu\text{molm}^{-2}\text{s}^{-1}$ of PAR intensity with BG-11 medium, except for nitrogen and phosphorous concentrations, 250 mgL^{-1} and 5.5 mgL^{-1} , respectively. A part of samples was taken at 6:00 (initial), 9:00, 12:00, 15:00, 18:00, 21:00, then was subjected to the analyses.

For both types, experimental units per each PAR and nutrient condition were triplicated in the same procedure, in order to confirm reproducibility.

Declarations

Acknowledgement

This work was financially supported by the Grant-in-Aid for Scientific Research (B) (19H02245) and the Fund for the Promotion of Joint International Research (18KK0116) of the Japan Society for the Promotion of Science (JSPS).

Author contribution statement

T.A. contributed to the design of the experiment, analyses, and writing the manuscript.

M.R. contributed to the revision of the manuscript.

H.D.L.A. carried out the experiment and writing the experiment part.

References

1. Barrington, D.J. & Ghadouani, A. Application of hydrogen peroxide for the removal of toxic cyanobacteria and other phytoplankton from waste water. *Environ. Sci. Technol.* **42**, 8916-8921 (2008)
2. Lurling, M., Meng, D. & Fassen, E.L. Effects of hydrogen peroxide and ultrasound on biomass reduction and toxin release in cyanobacterium, *Microcystis aeruginosa*. *Toxins* **6**, 3260-3281 (2014)
3. Cooper, W.J., Zika, R., Petasne, R.G. & Plane, J.M. Photochemical formation of hydrogen peroxide in natural waters exposed to sunPAR. *Environ. Sci. Technol.* **22**, 1156-1160. doi:10.1021/es00175a004 (1988)

4. Cooper, W.J., Lean, D.R.S. & Carey, J.H. Spatial and temporal patterns of hydrogen peroxide in lake waters. *Can. J. Fish. Aquat. Sci.* **46**, 1227-1231. doi: 10.1139/f89-158 (1989)
5. Cory, R.M. et al. Seasonal dynamics in dissolved organic matter, hydrogen peroxide, and cyanobacterial blooms in Lake Erie. *Frontiers in Marine Science*, doi: 10.3389/fmars.2016.00054 (2016)
6. Caverzan, A., Passaia, G., Rosa, S.B., Ribeiro, C.W., Lazzarotto, F. & Margis-Pinheiro, M Plant responses to stresses: role of ascorbate peroxidase in the antioxidant protection. *Genet. Mol. Biol.* **35**, 1011-1019 (2012)
7. Sharma, P., Jha, A.B., Dubey, R.S. & Pessarakli, M. Reactive oxygen species, oxidative damage, and antioxidative defense mechanism in plants under stressful conditions. *J. Botany.* (2012)
8. Ugya, A.Y., Imam, T.S., Li, A., Ma, J. & Hua, X. Antioxidant response mechanism of freshwater microalgae species to reactive oxygen species production: a mini review. *J. Chem. Ecol.* 1-20 (2019)
9. Rastogi, R.P., Singh, S.P., Häder, D.-P. & Sinha, R.P. Detection of reactive oxygen species (ROS) by the oxidant-sensing probe 2',7'-dichlorodihydrofluorescein diacetate in the cyanobacterium *Anabaena variabilis* PCC 7937. *Biochem. Biophys. Res. Commun.* **397**, 603-607 (2010)
10. Foyer, C.H. Reactive oxygen species, oxidative signaling and the regulation of photosynthesis. *Environ. Exp. Bot.* **154**, 134-142 (2018)
11. Gill, S.S. & Tuteja, N. Reactive oxygen species and antioxidant machinery in abiotic stress tolerance in crop plants. *Plant Physiol. Biochem.* **48**, 909-930 (2010)
12. Ma, Z. & Gao, K. Spiral breakage and photoinhibition of *Arthrospira platensis* (Cyanophyta) caused by accumulation of reactive oxygen species under solar radiation. *Environ. Exp. Bot.* **68**, 208-213 (2010)
13. Welkie, D.G. et al. A hard day's night: Cyanobacteria in Diel cycles. *Trends Microbiol.* **27**, 231-242 (2019)
14. Latifi, A., Ruiz, M. & Zhang, C.C. Oxidative stress in cyanobacteria. *FEMS Microbiol. Rev.* **33**, 258-278 (2009)
15. Lea-Smith, D.J., Bombelli, P., Vasudevan, R. & Howe, C.J. Photosynthetic, respiratory and extracellular electron transport pathways in cyanobacteria. *Biochimica et Biophysica Acta (BBA)-Bioenergetics* **1857**, 247-255 (2016)
16. Raja, V., Majeed, U., Kang, H., Andrabi, K.I. & John, R. Abiotic stress: Interplay between ROS, hormones and MAPKs. *Environ. Exp. Bot.* **137**, 142-157 (2017)

17. Asada, S., Fukuda, K., Oh, M., Hamanishi, C. & Tanaka, S. Effect of hydrogen peroxide on the metabolism of articular chondrocytes. *Inflamm. Res.* **48**, 399-403 (1999)
18. Nishiyama, Y. & Murata, N. Revised scheme for the mechanisms of photoinhibition and its application to enhance the abiotic stress tolerance of the photosynthetic machinery. *Appl. Microbiol. Biotechnol.* **98**, 8777-8796 (2014)
19. Mikula, P., Zezulka, S., Jancula, D. & Marsalek, B. Metabolic activity and membrane integrity changes in *Microcystis aeruginosa* – new findings on hydrogen peroxide toxicity in cyanobacteria. *Eur. J. Phycol.* **47**, 195-206 (2012)
20. Mittler, R. Abiotic stress, the field environment and stress combination. *Trends in plant science*, **11**, 15-19. doi:10.1016/j.tplants.2005.11.002 (2006)
21. Saints, M., Diaz, P., Monza, J. & Borsani, O. Heat stress results in loss of chloroplast Cu/Zn superoxide dismutase and increased damage to Photosystem II in combined drought-heat stressed *Lotus japonicus*. *Physiological Plantarum* **140**, 46-56. doi:10.1111/j.1399-3054.2010.01383.x (2010)
22. Suzuki, N., Rivero, R.M., Shulaev, V., Blumwald, E. & Mittler, R. Abiotic and biotic stress combinations. *New Phytologist* **203**, 3-43. doi:10.1111/nph.12797 (2014)
23. Asaeda, T. & Barnuevo, A. Oxidative stress as an indicator of niche-width preference of mangrove *Rhizophora stylosa*. *Forest Ecology and Management* **432**, 73-82 (2019)
24. Asaeda, T., Senavirathna, M.D.H.J., Vamsi Krishna, L. & Yoshida, N. Impact of regulated water levels on willows (*Salix subfragilis*) at a flood-control dam, and the use of hydrogen peroxide as an indicator of environmental stress. *Ecological Engineering*, **127**, 96-102 (2019)
25. Asaeda, T., Senavirathna, M.D.H.J. & Vamsi Krishna, L. Evaluation of habitat preference of invasive macrophyte *Egeria densa* in different channel slopes using hydrogen peroxide as an indicator. *Frontiers in Plant Science* **11**.422, doi:10.3389/fpls.2020.00422 (2020)
26. Diaz, J. & Plummer, S. Production of extracellular reactive oxygen species by phytoplankton: past and future directions. *J. Plankton Res.* **40**, 655-666 (2018)
27. Abeynayaka, H.D.L., Asaeda, T. & Kaneko, Y. Buoyancy limitation of filamentous cyanobacteria under prolonged pressure due to the gas vesicle collapse. *Env. Man.* **60**, 293-303 (2017)
28. Jana, S. & Choudhuri, M.A. Glycolate metabolism of three submersed aquatic angiosperms during ageing. *Aquatic Botany* **12**, 345–354 (1982)
29. Veljovic-Jovanovic S., Noctor G. & Foer C.H. Are leaf hydrogen peroxide concentrations commonly overestimated? The potential influence of artefactual interference by tissue phenolics and ascorbate. *Plant Physiology and Biochemistry* **28**, 318-327 (2002)

30. Cheeseman, J.M. Hydrogen peroxide concentrations in leaves under natural conditions. *J. Exp. Bot.* **57**, 2435-2444 (2006)
31. Queval, G., Hager J., Gakiere, B. & Noctor, G. Why are literature data for H₂O₂ contents so variable? A discussion of potential difficulties in the quantitative assay of leaf extracts. *J. Exp. Bot.* **59**, 135-146. doi:10.1093/jxb/em193 (2008)
32. Aebi, H. Catalase in vitro. *Methods in Enzymology* **105**, 121-126 (1984)
33. Nakano, Y. & Asada, K. Hydrogen peroxide is scavenged by ascorbate-specific peroxidase in spinach chloroplasts. *Plant Cell Physiol.* **22**, 867-880 (1981)
34. Ahmad, P., Jaleel, C.A., Salem, M.A., Nabi, G. & Sharma, S. Roles of enzymatic and non enzymatic antioxidants in plants during abiotic stress. *Cri. Rev. in Biotech.* **30**, 161-175 (2010)
35. Drábková, M., Admiraal, W. & Maršálek, B. Combined exposure to hydrogen peroxide and PAR – selective effects on cyanobacteria, green algae, and diatoms. *Environ. Sci. Technol.* **41**, 309-314 (2007a)
36. Bouchard, J.N. & Purdie, D.A. Effect of elevated temperature, darkness and hydrogen peroxide treatment on oxidative stress and cell death in the bloom-forming toxic cyanobacterium *Microcystis aeruginosa*. *J. Phycol.* **47**, 1316-1325 (2011)
37. Leunert, F., Eckert, W., Paul, A., Gerhardt, V. & Grossart, H.P. Phytoplanktonic response to UV-generated hydrogen peroxide from natural organic matter. *J. Plankton Res.* **36**, 185-197. doi:10.1093/plankt/fbt096 (2014)
38. Wang, B., Song, Q., Long, J., Song, G., Mi, W. & Bi, Y. Optimization method for *Microcystis* bloom mitigation by hydrogen peroxide and its stimulative effects on growth of chlorophytes. *Chemosphere* **228**, 503-512 (2019)
39. Foo, S.C., Chapman, I.J., Hartnell, D.M., Turner, A.D. & Franklin D.J. Effects of H₂O₂ on growth, metabolic activity and membrane integrity in three strains of *Microcystis aeruginosa*. *Env. Sci. Poll. Res.* **27**, 38916-38927 (2020)
40. Barrington, D.J., Reichwaldt, E.S. & Ghadouani, A. The use of hydrogen peroxide to remove cyanobacteria and microcystins from waste stabilization ponds and hypereutrophic systems. *Ecol. Engin.* **50**, 86-94 (2013)
41. Drábková, M., Matthijs, H., Admiraal, W. & Maršálek, B. Selective effects of H₂O₂ on cyanobacterial photosynthesis. *Photosynthetica.* **45**, 363-369 (2007b)

42. Cooper, W.J., Zika, R., Petasne, R.G. & Plane, J.M. Photochemical formation of hydrogen peroxide in natural waters exposed to sunPAR. *Environ. Sci. Technol.* **22**, 1156-1160. doi:10.1021/es00175a004 (1988)
43. Garcia, P.E., Queimalinos, C. & Dieguez, M.C. Natural levels and photo-production rates of hydrogen peroxide (H₂O₂) in Andean Patagonian aquatic systems: Influence of the dissolved organic matter pool. *Chemosphere*. **217**, 550-557 (2019)
44. Herrmann, R., 1996. The daily changing pattern of hydrogen peroxide in New Zealand surface waters. *Environm. Toxicol. & Chem.* **15**, 652-662.
45. Spooof, L. et al. Elimination of cyanobacteria and microcystins in irrigation water – Effects of hydrogen peroxide treatment. *Env. Sci. Poll. Res.* **27**, 8638-8652. doi.org/10.1007/s11356-019-07476-x (2020)
46. Lopez, C.V.G. et al. Protein measurements of microalgae and cyanobacterial biomass. *Bioresource Technol.* **101**, 7587-7591 (2010)
47. Vesterkvist, P.S.M., Misiorek, J.O., Spooof, L.E.M., Toivola, D.M. & Meriluoto, J.A.O. Comparative cellular toxicity of hydrophilic and hydrophobic Microcystins on Caco-2 Cells. *Toxins* **4**, 1008 (2012)
48. Preece, E.P., Hardy, F.J., Moore, B.C. & Bryan, M. A review of microcystin detections in estuarine and marine waters: Environmental implications and human health risk. *Harmful Algae* **61**, 31-45 (2017)
49. Pham, T.-L. & Utsumi, M. An overview of the accumulation of microcystins in aquatic ecosystems. *J. Environ. Manag.* **213**, 520-529 (2018)
50. Goldman, J.C., McCarthy, J.J., D.G. & Peavey, D.G. Growth rate influence on the chemical composition of phytoplankton in oceanic waters. *Nature* **279**, 210215 (1979)
51. Paerl, H.W., Fulton, R.S. 3rd, Moisander, P.H. & Dyble, J. Harmful freshwater algal blooms, with an emphasis on cyanobacteria. *Scient. World J.* **12805693**, PMC6083932 (2001)
52. Xie, L., Xie, P., Li, Sixin, Tang, H. & Liu, H. The low TN:TP ratio, a case or result of Microcystis blooms? *Water Res.* **37**, 2070-2080 (2003)
53. Asaeda, T., Rashid, Md.H., & Schoelynck, J. Tissue Hydrogen Peroxide Concentration Can Explain the Invasiveness of Aquatic Macrophytes: A Modeling Perspective. *Front. Environ. Sci.* **8**, (2021)
54. Hesse, K., Dittman, E., Borner, T., 2001. *FEMS microbiology ecology* **37**, 39-43.
55. Tilzer, M.M. Light dependence of photosynthesis and growth in cyanobacteria: Implications for their dominance in eutrophic lakes. *N. Z. J. Mar. Freshw. Res.* **21**, 401-412 (1987)

56. Iwase, S. & Abe, Y. Identification and change in concentration of musty-odor compounds during growth in blue-green algae. *J. School Mar. Sci. Tech.* **8**, 27-33 (2010)
57. Rippka, R., Deruelles, J., Waterbury, J.B., Herdman, M. & Stanier, R.Y. Generic assignments, strain histories and properties of pure cultures of cyanobacteria. *Microbiology* **111**, 1-61 (1979)

Figures

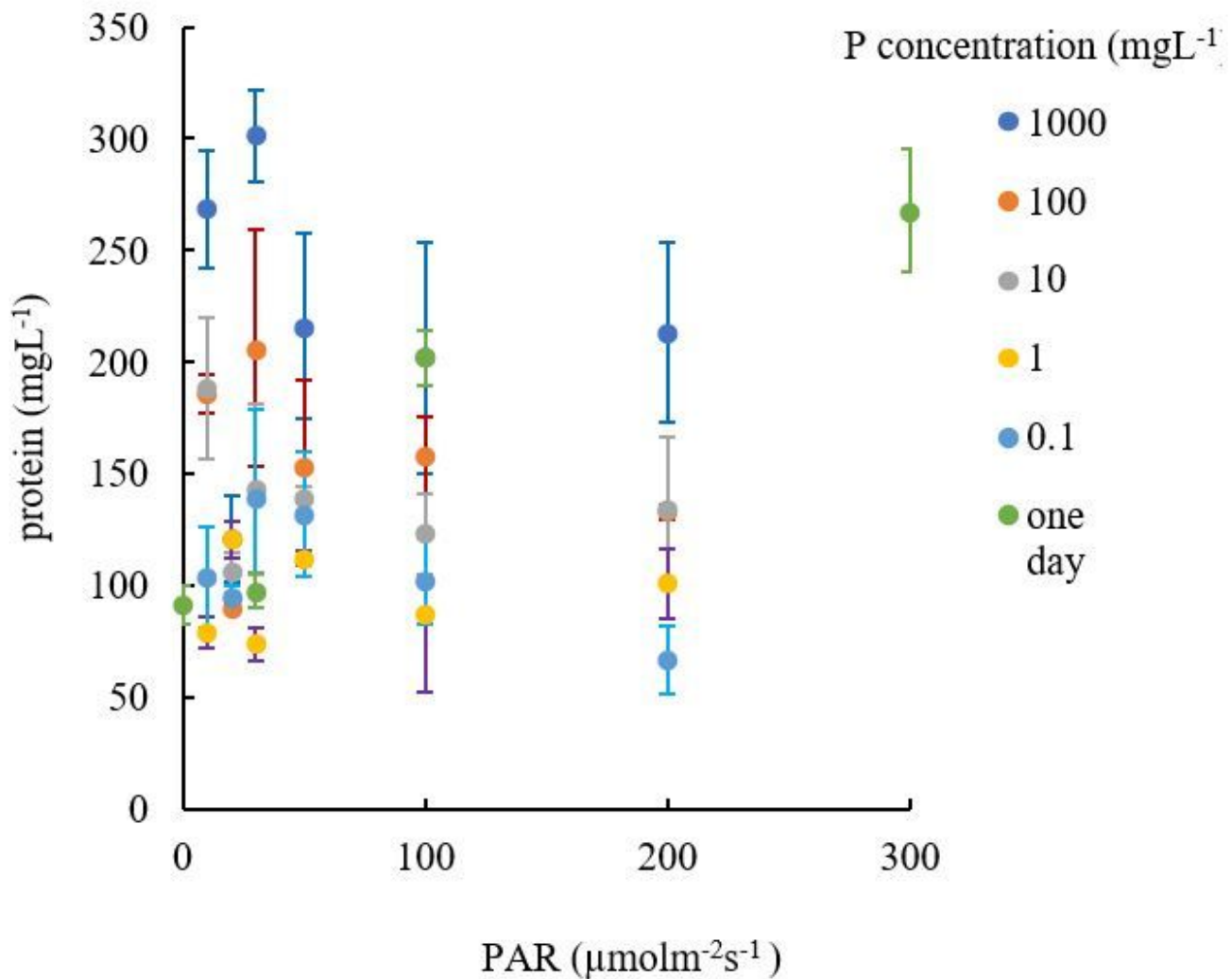


Figure 1

Protein content for different PAR intensity levels and for each phosphorus concentration level (mgL⁻¹). Vertical bars indicate standard deviation.

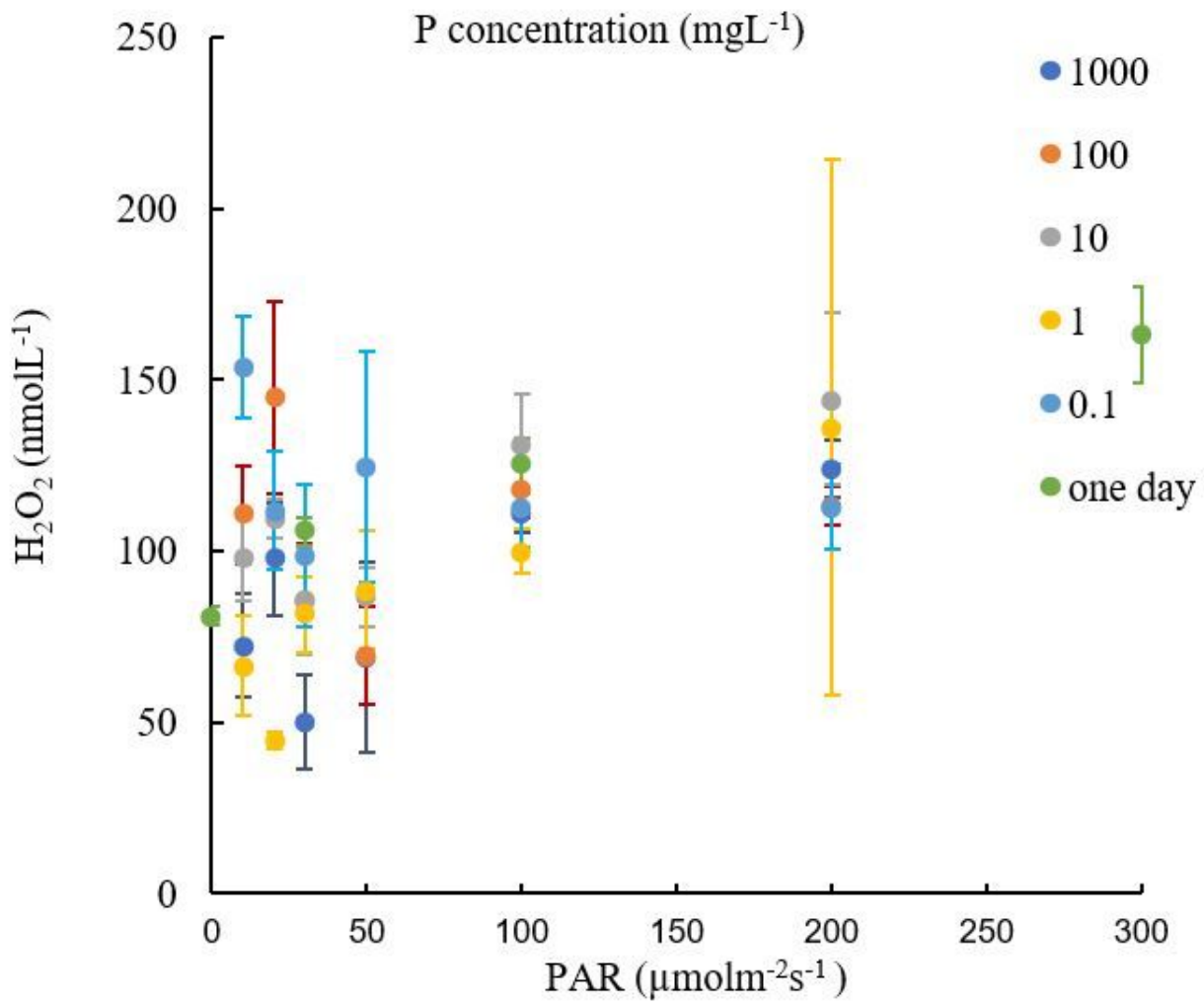


Figure 2

H₂O₂ concentration for different PAR intensity levels and for each phosphorus concentration level (mgL⁻¹). Vertical bars indicate standard deviation.

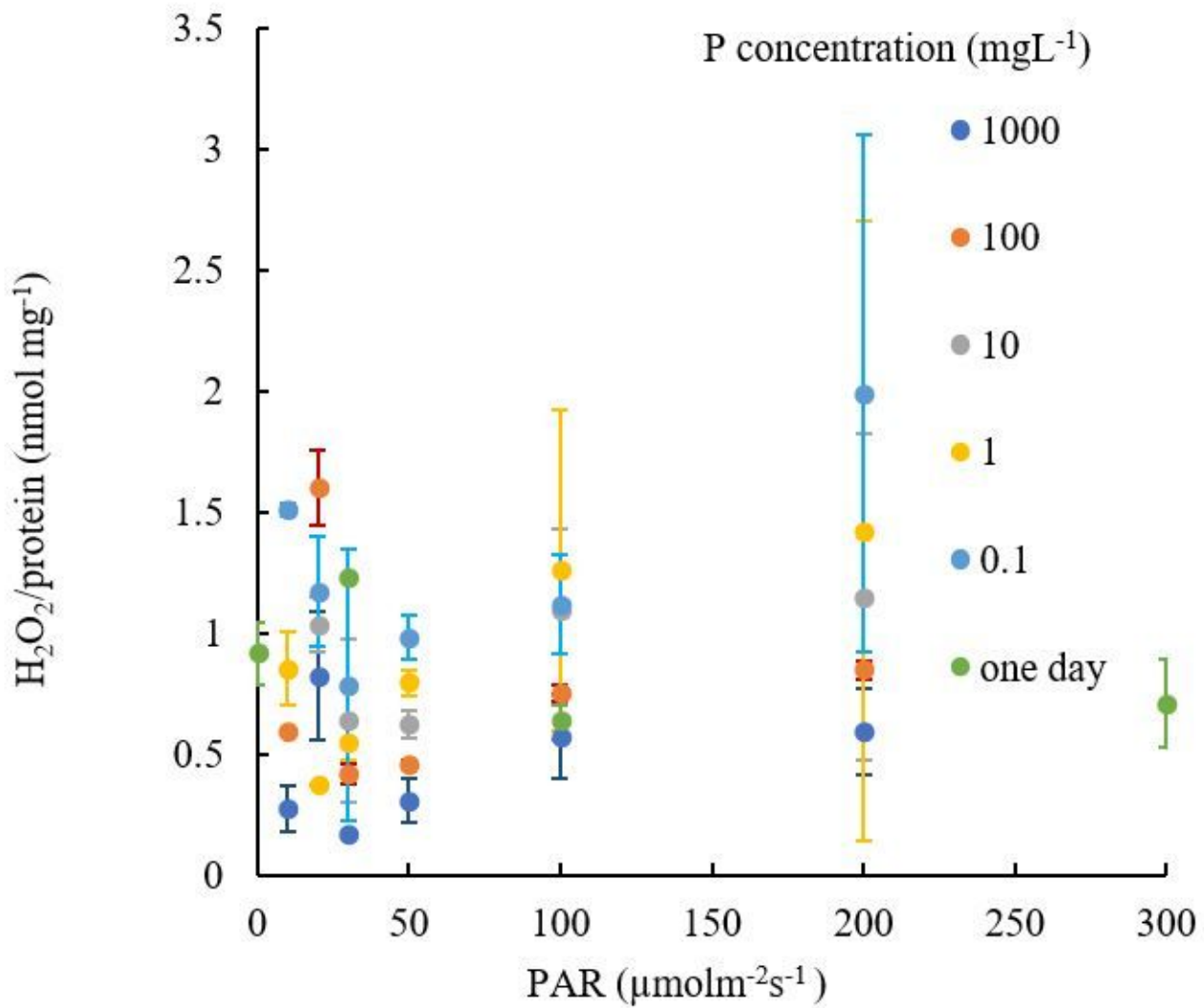


Figure 3

H₂O₂ content per protein for different PAR intensity levels and for each phosphorus concentration level (mgL⁻¹). Vertical bars indicate standard deviation.

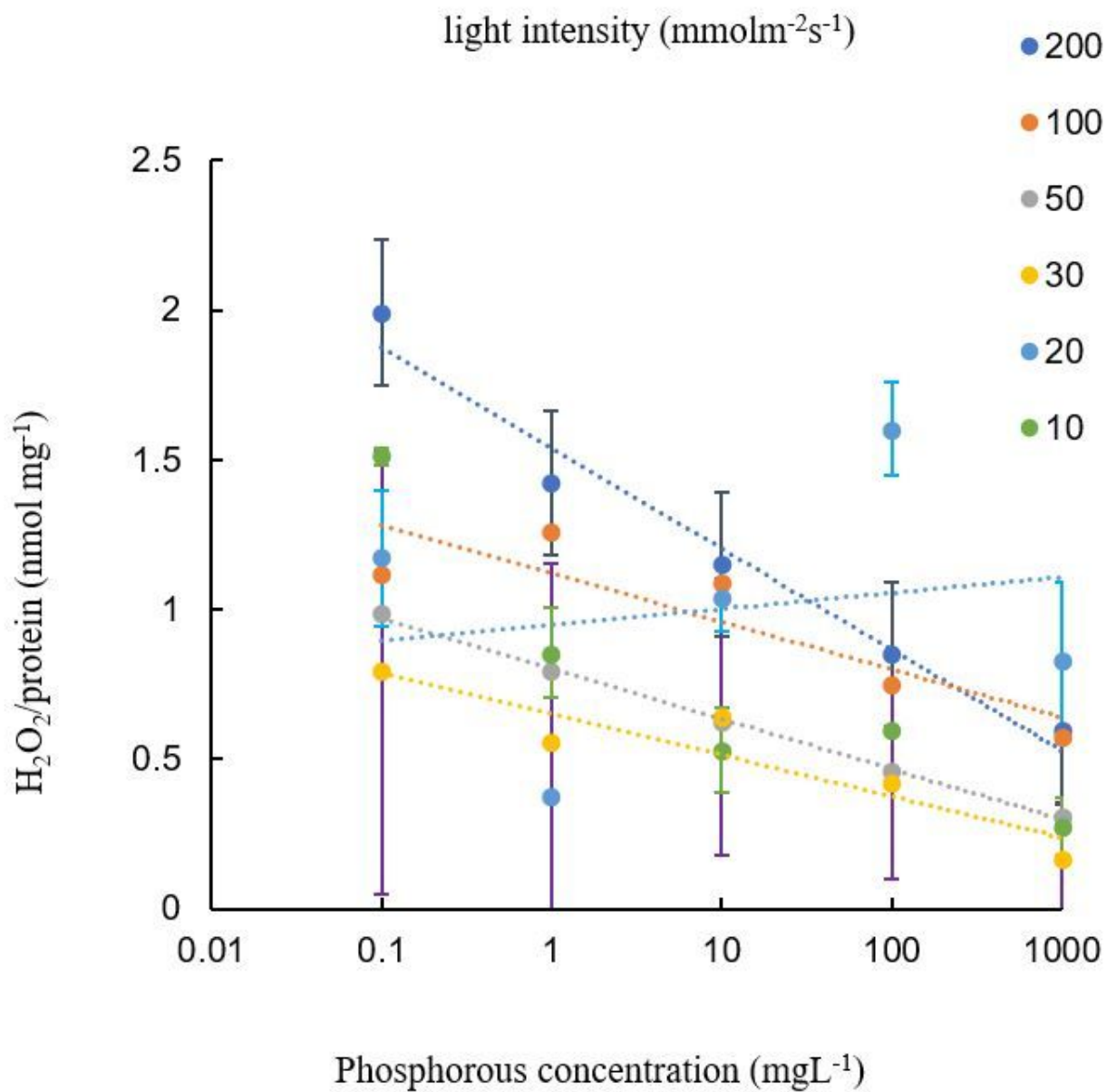


Figure 4

H_2O_2 content per protein for different phosphorus concentration level (mgL^{-1}) and for each PAR intensity level ($\mu\text{molm}^{-2}\text{s}^{-1}$). Vertical bars indicate standard deviation. Dotted lines show the approximate relation for each light intensity.

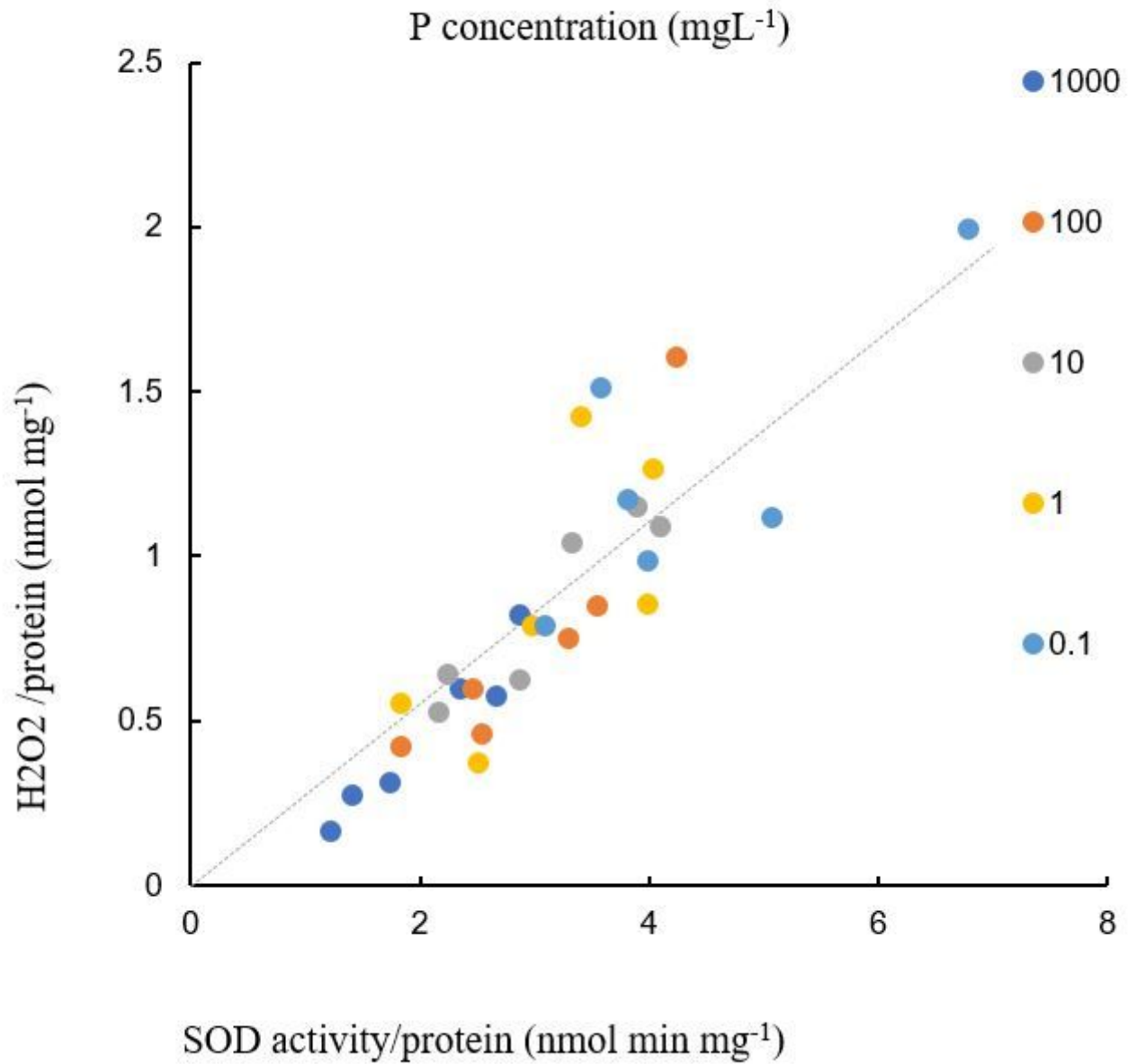


Figure 5

SOD activity per protein for different phosphorus concentration level (mgL⁻¹) and for each PAR intensity level (μmolm⁻²s⁻¹). The approximate relation is shown by the diagonal line.

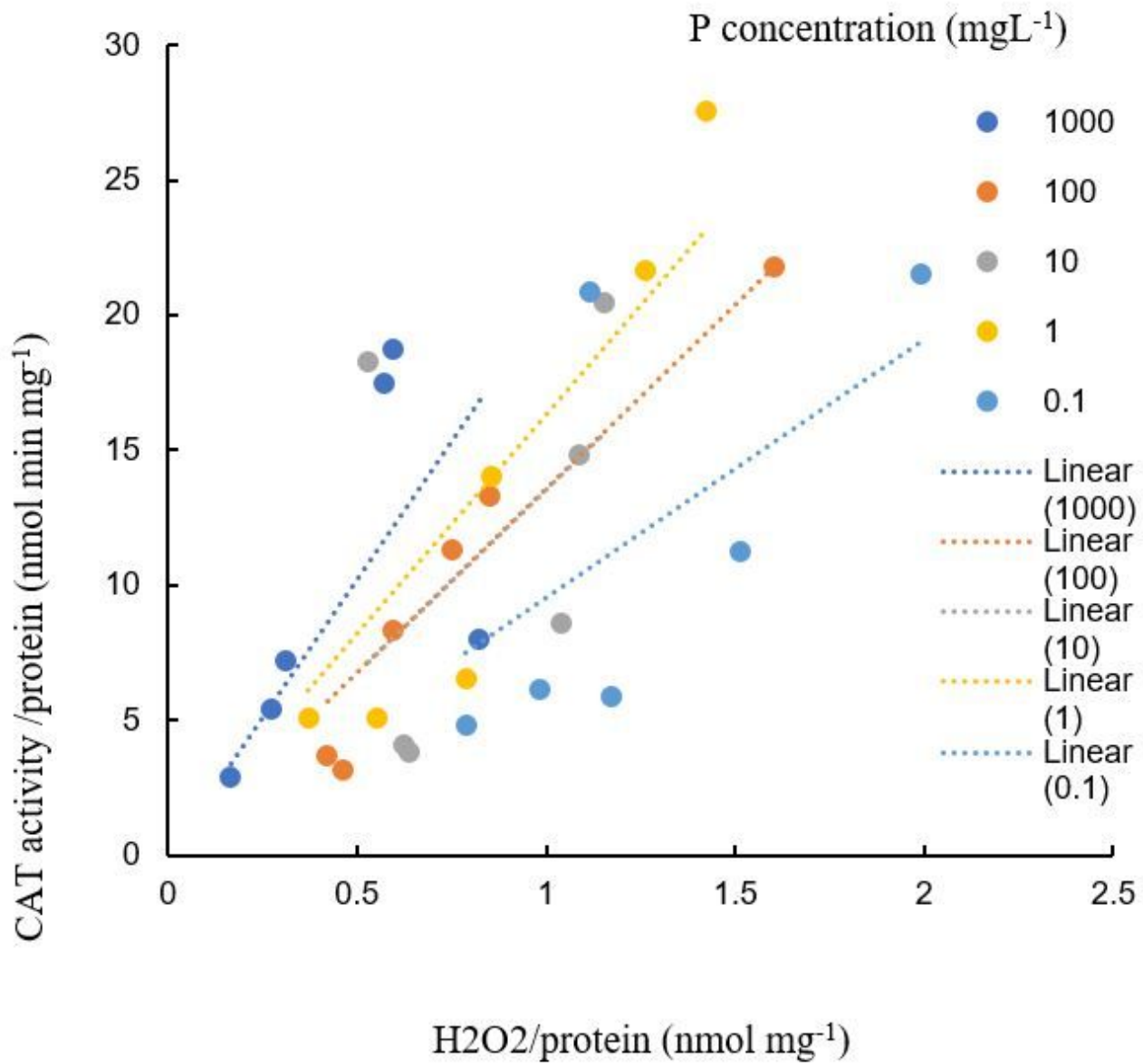


Figure 6

CAT activity per protein for different phosphorus concentration levels (mgL⁻¹) and for each PAR intensity level (μmolm⁻²s⁻¹). Dotted lines indicate the approximate lines for each phosphorus concentration.

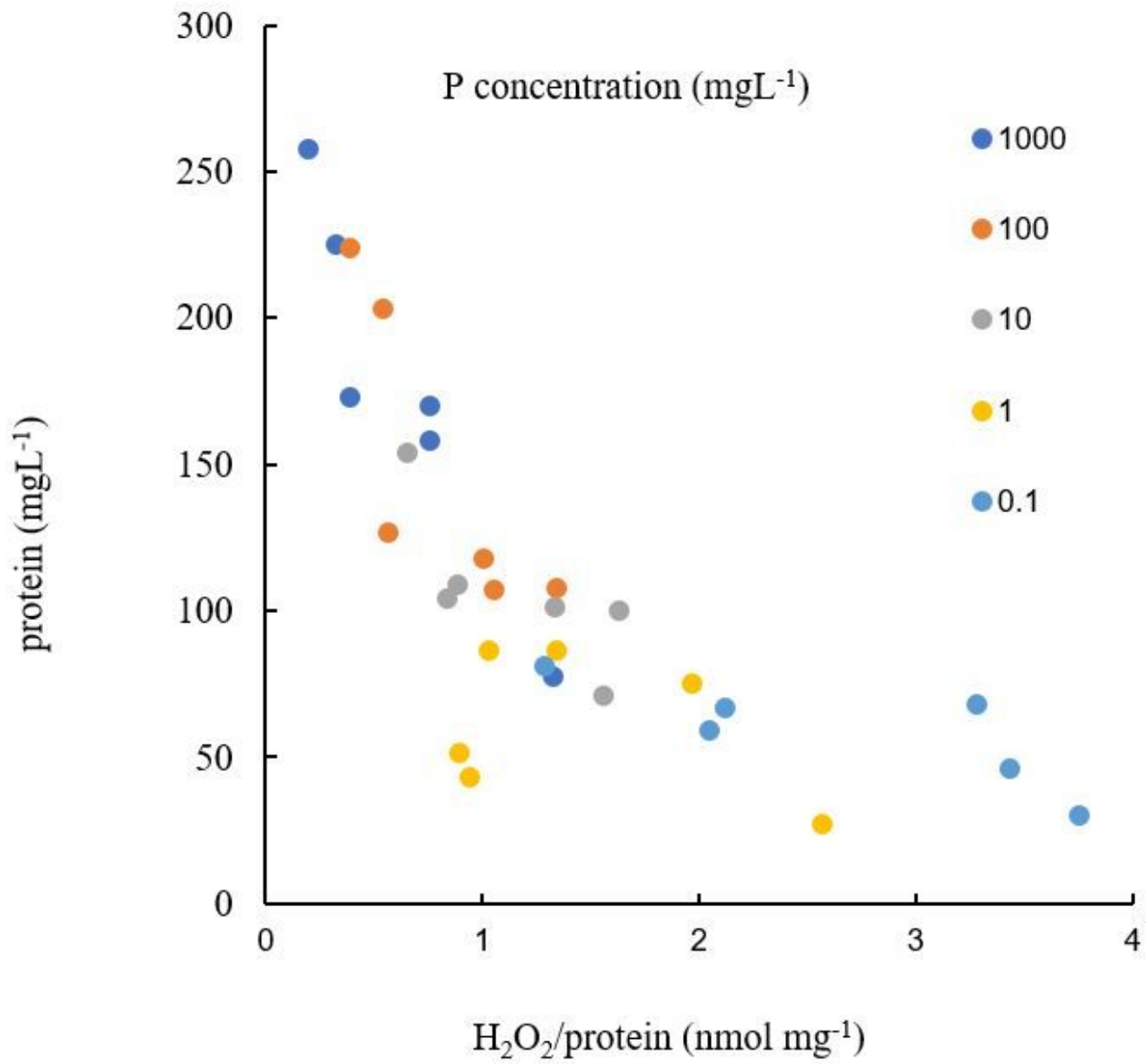


Figure 7

Protein content in water for different phosphorus concentration levels (mg/L) and for each PAR intensity level ($\mu\text{molm}^{-2}\text{s}^{-1}$)

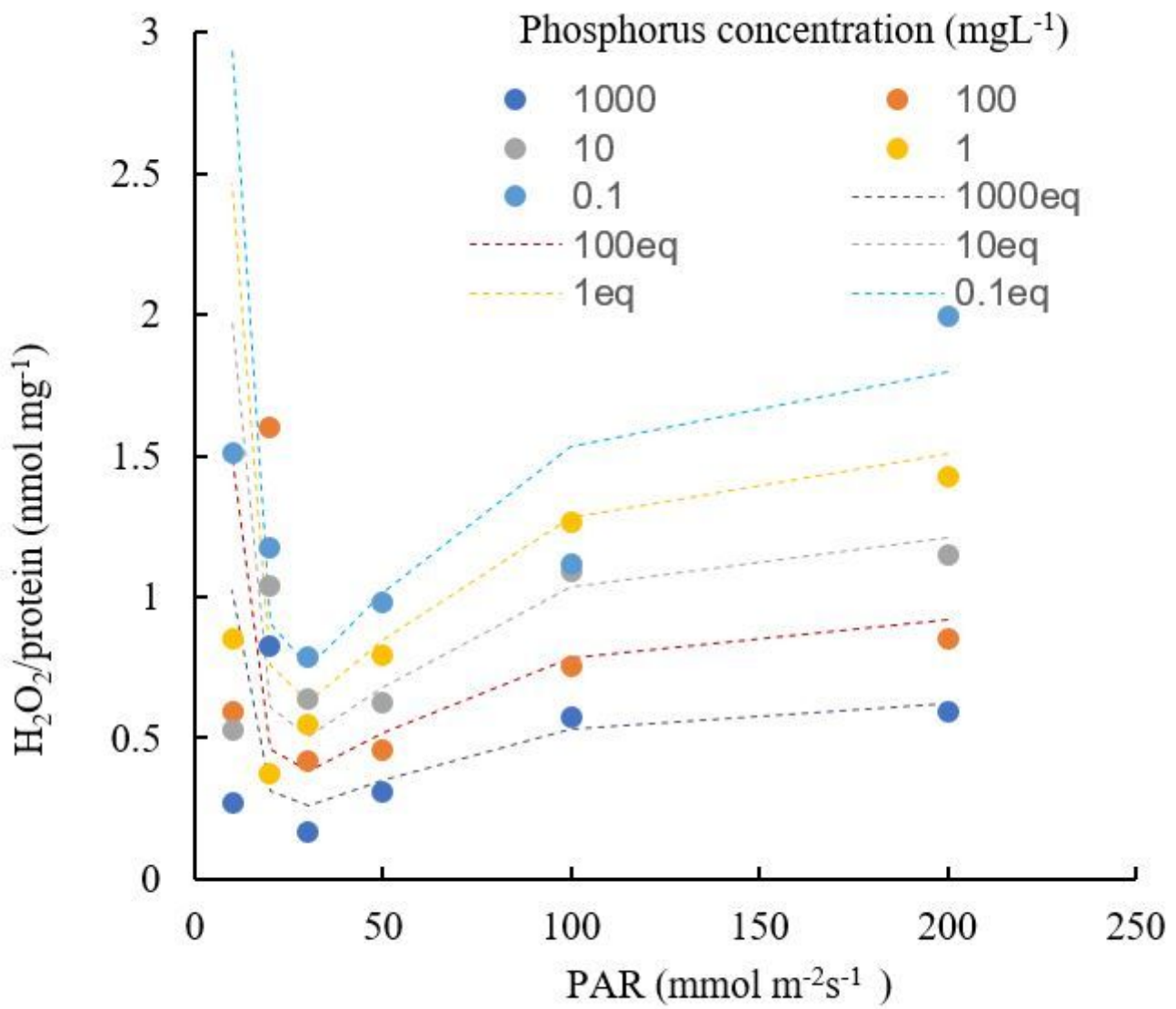


Figure 8

The simulated results of H₂O₂/protein by equation (1) compared with experimental results.

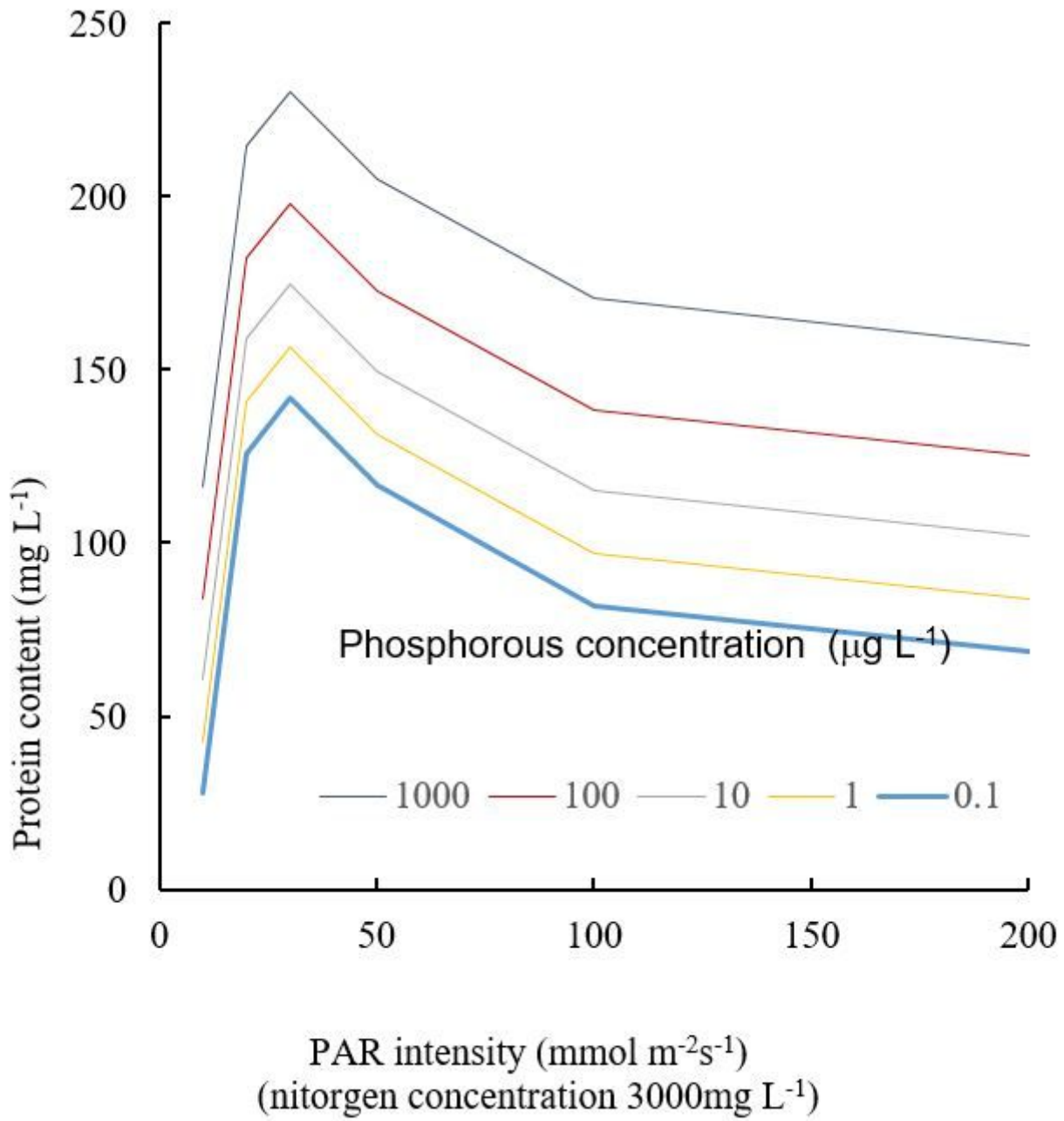


Figure 9

The simulated results of protein content by equation (2)